Journal of Structural Geology, Vol. 9, No. 7, pp. 809 to 817, 1987
Printed in Great Britain

0191-8141/87 $03.00 + 0.00

A model for the development of crenulations in shear zones with applications from the Southern Appalachian Piedmont

A. J. DENNIS and D. T. SECOR

Geology Department, University of South Carolina, Columbia, SC 29208, U.S.A.

(*Received* 31 *October* 1985; *accepted in revised form* 16 *February* 1987)

Abstract—Two sets of crenulations are associated with a major, Alleghanian, dextral shear zone which deformed stratigraphic and structural boundaries in the eastern Piedmont of South Carolina. Both sets of crenulation planes are oblique to the boundaries of the shear zone. The morphologies and orientations of the crenulation sets and their spatial distributions indicate that they are related to slip along foliation planes, and that they serve to compensate for displacement components of foliation slip normal to the overall movement direction in the shear zone. The crenulations act to maintain the initial thickness of the shear zone. Our evaluation of the recent literature on shear zones suggests that crenulations related to foliation slip are abundant and constitute a reliable sense of shear indicator.

INTRODUCTION

DEFORMATION WITHIN shear zones may be generalized into two dominant modes. Some structures form as a result of a marker's angular position within the strain ellipsoid. For example, if a layer is inclined such that it lies in the shortening space of the strain ellipsoid, it might buckle and fold; similarly, if a layer lies in the extending space of the strain ellipsoid, it might ductilely thin or boudin. Another mode of deformation involves slip on foliation and those structures that result from slip. The object of this paper is to examine the possible consequences of such slip. In the Irmo shear zone in the eastern Piedmont of South Carolina, lithologic and structural boundaries were intersected at a small angle by a 10 km wide, northeast-trending, dextral shear zone. Both compressional and extensional structures were formed as a result of this shearing. Two sets of crenulations were also formed in the shear zone. These crenulation sets are both oblique to the boundaries of the zone, and we believe that they formed as a consequence of slip on foliation. This paper describes our model for the formation of oblique crenulations in shear zones, and provides examples from the eastern Piedmont of South Carolina.

THE MODEL

We consider a dextral shear zone that is undergoing progressive simple shear displacement. The displacements are parallel to the x co-ordinate direction, and the zone walls are parallel to the x–z co-ordinate plane (Fig. 1). The width of the zone is constant with time. On a macroscopic scale, the material in the zone is homogeneously strained, and material outside is unstrained. Strain within the zone is related to the operation of three mechanisms.

(1) Material in the zone is assumed to be foliated. The foliation planes are perpendicular to the x–y plane and are inclined at a counterclockwise acute angle (α) to the x direction (Fig. 1). Dextral slip is occurring along foliation surfaces. Foliation slip is modelled as homogeneous simple shear with displacements parallel to both the x–y plane and the foliation planes. Foliation slip is assumed to be penetrative at both macroscopic and mesoscopic scales. The simple shear displacements acting parallel to foliation are inclined to the shear zone boundaries, and consequently foliation slip will tend to rotate the boundaries and increase the thickness of the zone (Fig. 2a). In order to maintain compatibility between material inside and outside the zone, we assume that the material inside undergoes a rigid body rotation which restores the zone boundaries to their original orientation (Fig. 2b) and we assume that slip is occurring along a crenulation in order to restore the zone to its original thickness (Fig. 2c).

(2) The crenulation planes are perpendicular to the x–y plane and are inclined at a clockwise acute angle (β) to the x direction (Fig. 1). On a macroscopic scale, crenulation slip is modelled as dextral homogeneous simple shear with all displacements parallel to both the x–y plane and the crenulation planes. On a mesoscopic scale, crenulation is not penetrative, and foliation planes between crenulation surfaces are not rotated as a result of crenulation slip. The displacements associated with crenulation slip are assumed to restore the shear zone to its original thickness. However, the boundaries of the

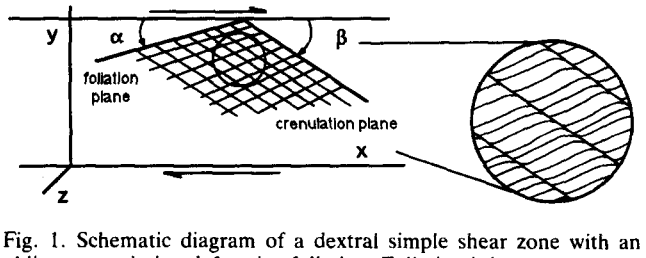

Fig. 1. Schematic diagram of a dextral simple shear zone with an oblique crenulation deforming foliation. Foliation is homogeneous at mesoscopic and macroscopic scales, whereas crenulation is homogeneous only to the mesoscopic scale.

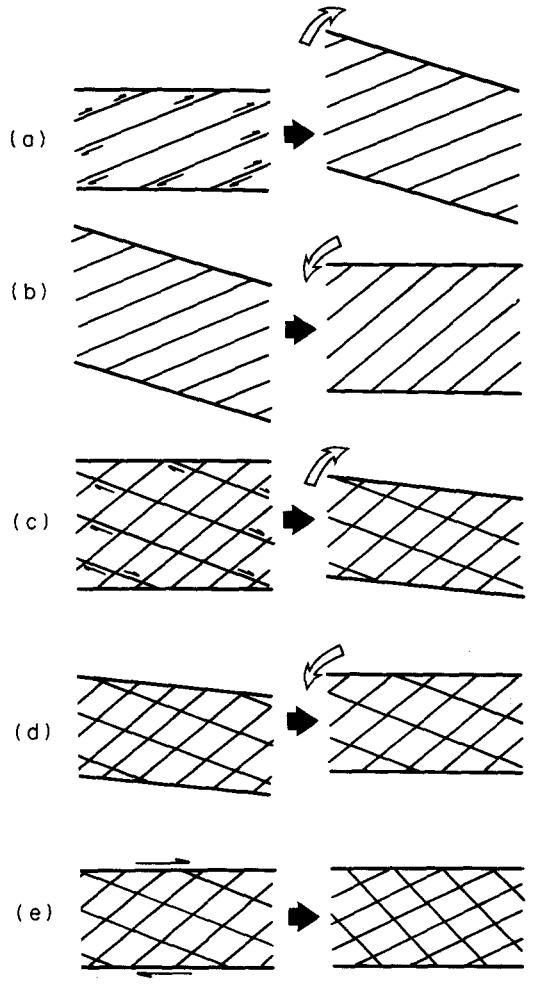

Fig. 2. (a) Dextral slip along foliation will rotate the shear zone boundaries clockwise and the thickness of the zone will increase. (b) A counterclockwise rigid body rotation may restore the zone boundaries to their original orientation. (c) Dextral slip along crenulation planes will rotate the shear zone boundaries clockwise and may reduce the zone to its original thickness. (d) A second counterclockwise back rotation may again restore zone boundaries to their original orientation. (e) The orientation of zone boundaries and zone thickness are unchanged by penetrative simple shear acting parallel to the shear direction. Foliation and crenulation are rotated by transformation **E**.

zone will rotate clockwise because crenulation displacements are inclined to zone boundaries (Fig. 2c). Consequently, we assume that material inside the zone undergoes a second rigid body rotation in order to maintain compatibility at the zone boundaries (Fig. 2d).

(3) In a subsequent mathematical analysis, we will show that the displacements involved in foliation and crenulation slip, along with the associated rigid body rotations, can be composed to give a megascopically homogeneous simple shear with all displacements parallel to the x co-ordinate direction. However, it is not necessary that all strain in the zone be related to foliation and crenulation slip. Therefore, we also assume that the material in the zone is undergoing a penetrative simple shear, with displacements parallel to x, that is homogeneous at macroscopic and mesoscopic scales (Fig. 2e). This might be a kinematic effect of oblique quartz grain shape fabrics (Lister & Snoke 1984) or asymmetric crystallographic fabrics. This third simple shear will rotate material planes inclined to the shear zone boundaries (such as foliation and crenulation) at the mesoscopic scale because it is homogeneous and penetrative at that scale.

It is well known that a given displacement can result from any one of an infinite variety of deformation paths. Cause and effect considerations outlined above suggest that the deformation path illustrated in Fig. 2 is possible. In the analysis which follows we assume this deformation path, however, at a later point we show that our results are independent of the order in which the increments of displacement are taken.

We now present an analysis of the deformation that takes place in the shear zone during a specific interval of time. During this interval, five successive increments of displacement corresponding to the five steps in the deformation path illustrated in Fig. 2, are assumed to take place. Each displacement increment is modelled as a linear transformation relating the positions of points before and after the increment. In this analysis, we use Roman numeral superscripts to indicate different stages in the deformation path. For example, x and y refer to the co-ordinates of points prior to deformation, x^{III} and y^{III} are co-ordinates following step III in the deformation path, and α^{V}, β^{V} refer to the orientations of foliation and crenulation following step V. In matrix notation, the transformations involved in the five steps of the deformation path can be represented as follows:

$$\mathbf{[A]} \quad \begin{bmatrix} x \\ y \end{bmatrix} = \begin{bmatrix} x^{I} \\ y^{I} \end{bmatrix} \tag{1}$$

$$\mathbf{[B]} \quad \begin{bmatrix} x^{I} \\ y^{I} \end{bmatrix} = \begin{bmatrix} x^{II} \\ y^{II} \end{bmatrix} \tag{2}$$

$$\mathbf{[C]} \quad \begin{bmatrix} x^{II} \\ y^{II} \end{bmatrix} = \begin{bmatrix} x^{III} \\ y^{III} \end{bmatrix} \tag{3}$$

$$\mathbf{[D]} \quad \begin{bmatrix} x^{III} \\ y^{III} \end{bmatrix} = \begin{bmatrix} x^{IV} \\ y^{IV} \end{bmatrix} \tag{4}$$

$$\mathbf{[E]} \quad \begin{bmatrix} x^{IV} \\ y^{IV} \end{bmatrix} = \begin{bmatrix} x^{V} \\ y^{V} \end{bmatrix}. \tag{5}$$

We now derive expressions for the transformation matrices **A–E** and the rotations of foliation and crenulation that take place during each displacement step.

Consider a foliation inclined at α (measured counter clockwise) to the shear zone boundary (Fig. 3). A simple

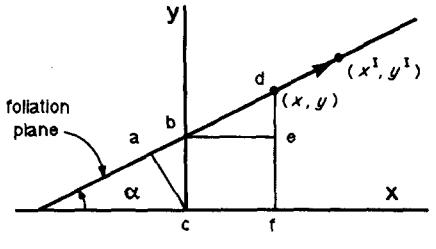

Fig. 3. Schematic diagram of simple shear along foliation in which the point (x,y) is displaced to (x^I, y^I) relative to the origin of the co-ordinate system. Construction lines are light. ac is perpendicular to foliation, be is parallel to the co-ordinate axis x, and df is parallel to y.

shear acts along the foliation and the point (x,y) is displaced to (x^I,y^I). γ is the shear strain of lines parallel and perpendicular to foliation. From Fig. 3:

$$\text{displacement of } (x,y) = \gamma \text{ ac} \tag{6}$$

$$\text{ac} = \text{bc} \cos \alpha \tag{7}$$

$$\text{bc} = y - x \tan \alpha \tag{8}$$

$$\text{ac} = (y - x \tan \alpha) \cos \alpha \tag{9}$$

$$\text{displacement of } (x,y) = \gamma(y - x \tan \alpha) \cos \alpha. \tag{10}$$

The components of displacement in the x and y directions will be, respectively:

$$\gamma (y - x \tan \alpha) \cos^2 \alpha \tag{11}$$

$$\gamma (y - x \tan \alpha) \sin \alpha \cos \alpha. \tag{12}$$

Making trigonometric substitutions, the following transformation equations are obtained from step I of the deformation path:

$$(1 - \gamma \sin \alpha \cos \alpha)\, x + \gamma \cos^2 \alpha\, y = x^I \tag{13}$$

$$-\gamma \sin^2 \alpha\, x + (1 + \gamma \sin \alpha \cos \alpha)\, y = y^I. \tag{14}$$

The entries of **A** (a_{ij}) are therefore:

$$a_{11} = 1 - \gamma \sin \alpha \cos \alpha \tag{15}$$

$$a_{12} = \gamma \cos^2 \alpha \tag{16}$$

$$a_{21} = -\gamma \sin^2 \alpha \tag{17}$$

$$a_{22} = 1 + \gamma \sin \alpha \cos \alpha. \tag{18}$$

The displacements of the foliation slip are parallel to foliation, and the foliation is not rotated:

$$\alpha = \alpha^I. \tag{19}$$

The orientation of crenulation following transformation **A** is obtained by inverting (13) and (14) and setting $y = -\tan \beta\,(x)$:

$$\beta^I = \arctan \{[\gamma \sin^2 \alpha + \tan \beta\,(1 + \gamma \sin \alpha \cos \alpha)]/ [1 - \gamma \sin \alpha \cos \alpha + \gamma \cos^2 \alpha \tan \beta]\}. \tag{20}$$

The rigid body rotation required in step II of the deformation path (ω^{II}) will be equal in magnitude and of opposite sense to the rotation of the shear zone boundary (i.e. the plane $y = 0$) in step I. The amount of forward rotation of the shear zone boundary by transformation **A** is obtained by inverting (13) and (14) and setting $y = 0$:

$$\tan (\omega^{II}) = +\gamma \sin^2 \alpha \,/\, (1 - \gamma \sin \alpha \cos \alpha) = -a_{21}/a_{11}. \tag{21}$$

The transformation equations for a counterclockwise rotation (ω^{II}) can be written as follows:

$$\cos \omega^{II} x^I - \sin \omega^{II} y^I = x^{II} \tag{22}$$

$$\sin \omega^{II} x^I + \cos \omega^{II} y^I = y^{II}. \tag{23}$$

Substituting (20) in (22) and (23), the back rotation transformation matrix **B** can be written:

$$[\mathbf{B}] = h_a \begin{bmatrix} a_{11} & a_{21} \\ -a_{21} & a_{11} \end{bmatrix}, \tag{24}$$

where (Fig. 4):

$$h_a = +\,(a_{11}^2 + a_{21}^2)^{-\frac{1}{2}}. \tag{25}$$

The orientations of foliation and crenulation following transformation **B** will be:

$$\alpha^{II} = \alpha + \omega^{II} \tag{26}$$

$$\beta^{II} = \beta^I - \omega^{II}. \tag{27}$$

Derivations analogous to those already given yield the following expressions for the entries of crenulation slip transformation **C**:

$$c_{11} = 1 + \psi \sin \beta^{II} \cos \beta^{II} \tag{28}$$

$$c_{12} = \psi \cos^2 \beta^{II} \tag{29}$$

$$c_{21} = -\psi \sin^2 \beta^{II} \tag{30}$$

$$c_{22} = 1 - \psi \sin \beta^{II} \cos \beta^{II}, \tag{31}$$

where ψ is the shear strain of lines parallel and perpendicular to crenulation at the beginning of step III of the deformation path. The displacements in step III are parallel to crenulation and therefore the crenulation does not rotate:

$$\beta^{II} = \beta^{III}. \tag{32}$$

Similarly, the foliation does not rotate during step III because the crenulation is not penetrative at the mesoscopic sale:

$$\alpha^{II} = \alpha^{III}. \tag{33}$$

By analogy with (21), the counterclockwise rigid body rotation (ω^{IV}) during **D** is given by:

$$\tan (\omega^{IV}) = -c_{21}/c_{11}. \tag{34}$$

By analogy with (24), the expression for back rotation transformation **D** is:

$$[\mathbf{D}] = h_c \begin{bmatrix} c_{11} & c_{21} \\ -c_{21} & c_{11} \end{bmatrix}, \tag{35}$$

where:

$$h_c = (c_{11}^2 + c_{21}^2)^{-\frac{1}{2}}. \tag{36}$$

The expressions for the foliation and crenulation orientations following **D** are, respectively:

$$\alpha^{IV} = \alpha^{III} + \omega^{IV} \tag{37}$$

$$\beta^{IV} = \beta^{III} - \omega^{IV}. \tag{38}$$

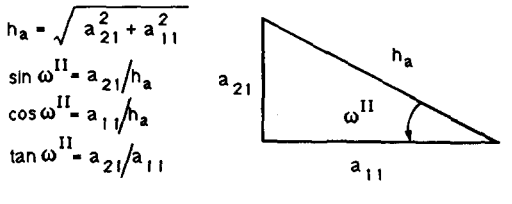

Fig. 4. See text for explanation.

The transformation matrix for a simple shear with displacements parallel to x (step V of the deformation path) is

$$[\mathbf{E}] = \begin{bmatrix} 1 & e_{12} \\ 0 & 1 \end{bmatrix}, \tag{39}$$

where e_{12} is the shear strain of lines parallel to the co-ordinate axes. The orientation of foliation (α^{V}) following the penetrative simple shear is obtained by inverting the transformation equations and setting $y^{IV} = \tan \alpha^{IV}(x^{IV})$:

$$\tan \alpha^{V} = \tan \alpha^{IV}/(1 + e_{12} \tan \alpha^{IV}). \tag{40}$$

Similarly, the orientation of crenulation (β^{V}) is:

$$\tan \beta^{V} = \tan \beta^{IV}/(1 - e_{12} \tan \beta^{IV}). \tag{41}$$

An expression for the overall transformation from the undeformed state through step V of the deformation path is obtained by composing the transformation matrices by taking their dot product:

$$[\mathbf{E}]\,[\mathbf{D}]\,[\mathbf{C}]\,[\mathbf{B}]\,[\mathbf{A}] \begin{bmatrix} x \\ y \end{bmatrix} = [\mathbf{F}] \begin{bmatrix} x \\ y \end{bmatrix} = \begin{bmatrix} x^{V} \\ y^{V} \end{bmatrix}. \tag{42}$$

The entries of the overall transformation matrix **F** are as follows:

$$f_{11} = h_a\, h_c \tag{43}$$

$$f_{12} = \{1/(h_a\, h_c)\}\{k_1 + k_1 \psi \sin \beta^{II}(2 \cos \beta^{II} + \psi \sin \beta^{II}) + k_2\} + e_{12} \tag{44}$$

$$f_{21} = 0 \qquad f_{22} = 1/(h_a\, h_c), \tag{45}$$

where

$$k_1 = \gamma \cos 2\alpha - \gamma^2 (\sin 2\alpha)/2 \tag{46}$$

$$k_2 = (\psi \cos 2\beta^{II} + \psi^2)/2. \tag{47}$$

If the overall transformation is a simple shear with displacement in the x–y plane and parallel to x, f_{11} and f_{22} both must be equal to one, and therefore:

$$h_a\, h_c = 1. \tag{48}$$

Substituting (25) and (36) in (48):

$$1 + \psi^2 \sin^2 \beta^{II} + \psi \sin 2\beta^{II} = 1/(1 + \gamma^2 \sin^2 \alpha - \gamma \sin 2\alpha) \tag{49}$$

and:

$$[\mathbf{F}] = \begin{bmatrix} 1 & f_{12} \\ 0 & 1 \end{bmatrix}. \tag{50}$$

Equation (49) constrains the orientation (β^{II}) and shear strain (ψ) of crenulations which form to compensate for components of foliation slip normal to the shear zone boundaries. Theory does not predict unique values for β^{II} and ψ, but if one is fixed, the other is determined by (49).

The above deformation path consists of a sequence of displacements that might take place during an interval of time in a zone of progressive homogeneous simple shear. Until now, no assumptions regarding the magnitudes of the shear strains involved in the displacement steps have been made. If the shear strains involved in steps I and III of the deformation path are finite, then finite but temporary changes in the orientation and thickness of the shear zone will occur. It seems likely that only under very special circumstances will such finite temporary changes be compatible with the natural boundary constraints controlling the overall geometry of the zone. A more reasonable model is one in which the displacement steps are infinitesimal, producing only infinitesimal changes in orientation and thickness of the zone. If infinitesimal displacement steps are assumed, the entries of **F** become:

$$f_{11} = 1 + 2\psi \sin \beta \cos \beta - 2\gamma \sin \alpha \cos \alpha \tag{51}$$

$$f_{12} = \psi(\cos^2 \beta - \sin^2 \beta) + \gamma(\cos^2 \alpha - \sin^2 \alpha) + e_{12} \tag{52}$$

$$f_{21} = 0 \tag{53}$$

$$f_{22} = 1/(1 + 2\psi \sin \beta \cos \beta - 2\gamma \sin \alpha \cos \alpha). \tag{54}$$

While cause and effect considerations dictate that the back rotations **B** and **D** do not precede their respective slip transformations **A** and **C**, an effect of the infinitesimal displacement assumption is that the entries of **F** are independent of the order in which **A**, **B**, **C**, **D** and **E** are composed; i.e. that once the crenulations are nucleated, the order in which foliation slip, crenulation slip and penetrative simple shear parallel to the shear direction are taken is not important so long as each occurs in a given interval **F**.

If infinitesimal displacement steps are assumed, (49) becomes:

$$(\gamma \cos \alpha) \sin \alpha = (\psi \cos \beta) \sin \beta. \tag{55}$$

For points on the plane $x = 0$, the first quantity in parentheses in (55) can be interpreted as the magnitude of a *foliation slip vector*, parallel and proportional to the displacement along the foliation in step I of the deformation path. Similarly, the second quantity in parentheses represents the magnitude of the *crenulation slip vector*. Therefore (55) indicates that the crenulation slip vector must add to the foliation slip vector to yield a vector parallel to the overall displacement of the shear zone (Fig. 5).

In the above model, both clockwise and counterclockwise rotations of foliation and crenulation occur at different stages in the deformation path. Foliation slip (transformation **A**) rotates crenulation planes clockwise because foliation is penetrative at the mesoscopic scale, whereas crenulation slip (transformation **C**) does not

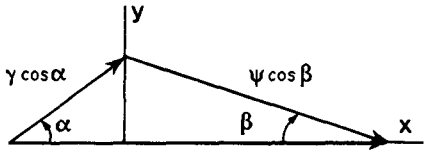

Fig. 5. The crenulation slip vector ($\psi \cos \beta$) compensates for the y component of the foliation slip vector ($\gamma \cos \alpha$), yielding a net slip vector parallel to the shear direction x.

rotate foliation because crenulation is not penetrative at the mesoscopic scale. This phenomenon is responsible for the common observation in sheared pelitic schists that foliation is apparently back rotated between crenulation surfaces so that foliation intersects crenulation at a relatively high angle. This apparent back rotation is an artifact of the scale to which foliation and foliation slip are penetrative relative to the scale to which crenulation and crenulation slip are penetrative. Both foliation and crenulation experience equal counterclockwise rigid body rotations during the back rotations **B** and **D**. The clockwise rotations of foliation and crenulation during the penetrative simple shear transformation **E** depends on the initial orientation of each. In both the finite and infinitesimal models presented above, the net rotations experienced by foliation and crenulation will be different from each other, and both clockwise and/or counterclockwise net rotations are possible.

In the preceding model, the overall transformation (**F**) was assumed to represent an infinitesimal simple shear with all displacements parallel to the x axis. The matrix entry f_{12} represents the net shear strain, during a specific interval of time, of lines originally parallel to co-ordinate axes x and y. Additional increments of infinitesimal shear strain may accumulate both prior to and following the specific time interval under consideration. If the net displacements during other time intervals are parallel to x, the finite shear strain may be obtained by numerical addition of the f_{12} entries. In this way, a large number of consecutive infinitesimal shear strains may be added to yield a finite simple shear with displacements parallel to x. The orientation of the shear zone boundaries remains constant; however, finite simple shear strains may accumulate along foliation and crenulation, and finite rotations of foliation and crenulation may take place.

In the preceding model, a dextral shear zone was assumed, and the foliation was oriented at a counterclockwise acute angle to the positive x direction (Fig. 1). A model for a sinistral shear zone would be exactly analogous to that already presented. It is also possible that a dextral shear zone might develop in a rock sequence where the original foliation was oriented at a clockwise acute angle to the positive x direction. In this case we predict that crenulation planes would develop in order to compensate for displacement components of foliation slip normal to the shear zone boundary, and that these crenulation planes would be oriented at a counterclockwise acute angle to the positive x direction. The geometric characteristics of crenulations that develop as a consequence of foliation slip in simple shear zones are considered in greater detail in the following section.

We now discuss four important special cases which are based on our field observations (Fig. 6). When the foliation is inclined at an acute angle, measured

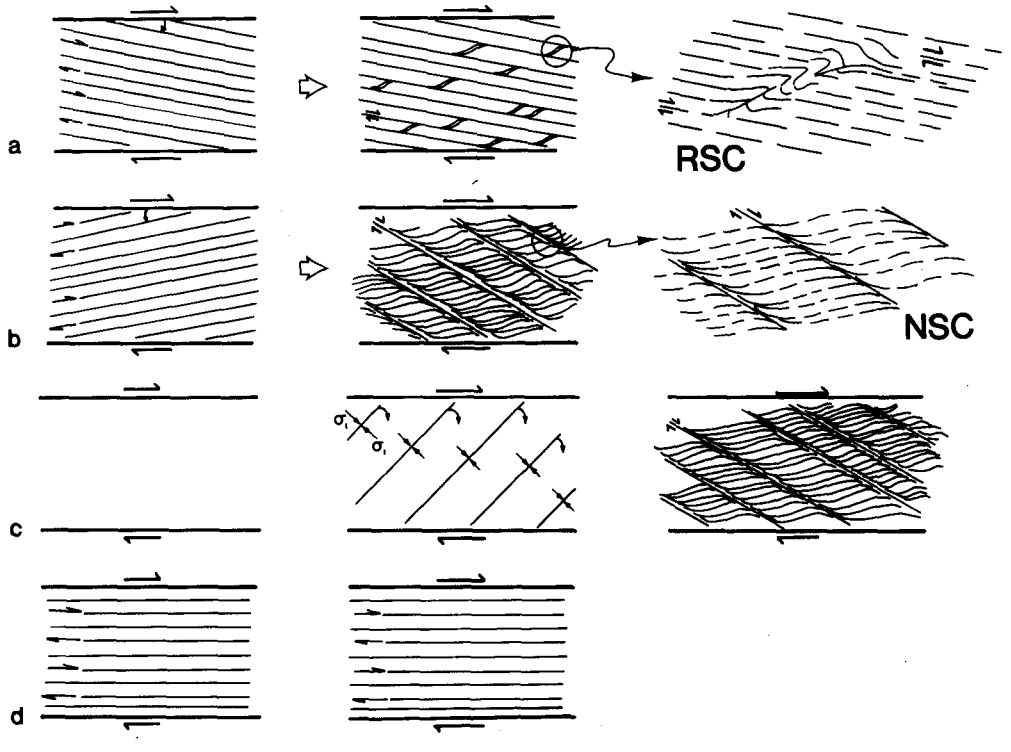

Fig. 6. Stylized development of oblique crenulations in shear zones: (a) development of reverse slip crenulations (RSC) compensates for movement normal to shear zone walls in systems where foliation is inclined at a clockwise acute angle to the shear zone movement direction, (b) development of normal slip crenulations (NSC) compensates for normal movement when foliation is inclined at a counterclockwise acute angle to x, (c) shearing of a foliation perpendicular to the cumulative flattening direction. If during progressive simple shearing this foliation is rotated into an easy slip orientation, and slip on foliation is an important mode of strain in the shear zone, then NSC will develop, (d) if the foliation is parallel to shear zone walls, then no compensating mechanism is required.

clockwise, to the shear zone movement direction (Fig. 6a), movement along that foliation normal to the shear zone boundaries must be compensated. Slip is transferred 'up' to 'higher' foliation planes by *reverse slip crenulations* (RSC). Reverse slip crenulations are rootless, intrafolial folds of foliation contained within lens-shaped pods with the same vergence sense as the main shear zone. The rootless aspect of these folds is controlled by microfaults that grow out of the foliation detachment surface. A penetrative simple shear parallel to the shear direction (transformation **E**) can result in a fabric that is approximately axial planar to RSC, but that is not genetically related to the mechanism that formed the crenulation fold. Movement normal to the shear zone boundary that is the result of slip along foliation oriented at a counterclockwise acute angle to x is compensated for by *normal slip crenulations* (NSC) (Fig. 6b). Normal slip crenulations offset the foliation in a normal sense that is synthetic with that of the main zone. Progressive simple shearing of a homogenous, isotropic substance may produce a foliation perpendicular to the cumulative flattening direction (Fig. 6c). Others have treated this problem (Lister & Williams 1979). As this foliation develops and rotates, slip along it may become possible and it assumes the clockwise acute case with the development of NSC surfaces. So while a foliation and a crenulation may form in the same deformation, it is not necessary for them to. If the foliation along which slip occurs is parallel to the shear plane, then no induced system is necessary (Fig. 6d), although minor perturbations in the orientation of the foliation or lithologic inhomogeneities might induce crenulations even in the case illustrated in Fig. 6(d). The cases described are simple models helpful conceptually in recognizing the angular relationships in simple shear systems where slip has occurred on a foliation inclined to the shear zone boundary, and a compensating mechanism is required for the component of movement normal to the overall displacement direction in the shear zone. It should be noted that the development of NSC or RSC may tend to inhibit further slip along the foliation in all of the cases described above.

THE IRMO SHEAR ZONE

In the eastern Piedmont of South Carolina, the Modoc Zone is a complex subvertical boundary between the greenschist grade Carolina slate belt in the northwest and the amphibolite facies Kiokee Belt to the southeast (Fig. 7a). In the area's most recent ductile deformation, the Modoc Zone was offset in a dextral sense across the 10 km wide Irmo shear zone. Whole rock and mineral radiometric ages suggest Irmo shear zone movement during the period 290–268 Ma (Dallmeyer *et al.* 1986). Most of the rocks affected by the Irmo shear zone contained foliations resulting from earlier deformations. Structural boundaries and foliations are subparallel to lithologic boundaries in the study area, so an approximate idea of the attitude of the foliation is suggested by the orientation of the mapped units. The boundaries of the Irmo shear zone illustrated in Fig. 7(b) were drawn using both the extent of units inferred to have been refolded by the shear zone and the observed distributions of NSC, RSC and *S* foliation developed in previously undeformed granitic rocks. Additional information on the structure and geologic history of the study area is available in Secor & Snoke (1978), Snoke *et al.* (1980) and Secor *et al.* (1986).

Several lines of evidence indicate that dextral slip has taken place along the dominant foliation in the Irmo shear zone. In thin section, small quartz veins which cross foliation at a high angle are consistently offset dextrally by slip surfaces coincident with foliation. These offsets do not seem proportional to the thickness of pelitic layering. Similarly, mesoscopic pegmatite dikes crossing the foliation at a high angle are dextrally offset. In deformed granitic rocks, feldspar porphyroclasts have trails of recrystallized material indicating dextral slip along the associated foliation (Snoke & Secor 1983). RSCs are observed to result from slip surfaces that 'ramp' from one set of foliation planes to another (Fig. 8).

In addition to the observed morphology of RSCs, other observational evidence also indicates a genetic relationship between the development of oblique crenulations and foliation slip. RSC and NSC are best developed in rocks having a strong planar fabric defined by orientation of (001) cleavage surfaces in mica, and the orientations of RSC and NSC vary sympathetically with the orientations of the dominant slip foliation. Passchier (1984) also recognized that orientation of NSC varies with the orientation of the dominant slip foliation.

The locations where measurements of axial surfaces and axes of RSC were made are shown in Fig. 7(c) & (d). Corresponding synoptic plots of these data are shown in Fig. 9(a) & (d). The dextral vergence of RSC and the average steeply plunging orientation of RSC axes indicate formation in a steeply dipping dextral shear zone undergoing approximately horizontal displacement. RSC folds are best developed in thinly laminated, flaser-bedded sandstones with thin pelitic drapes. Development of an early tectonic cleavage enhances the pelitic seams, and strain discontinuities (Lister & Williams 1983) and slip is common across such seams. In metavolcanic rocks, RSC typically occurs as mesoscopic cascades of dextral-verging chevrons. Quartz mineralization in the hinges of some of these chevrons is associated with dextral microfaulting along the limb that is being extended. Microfaults grow out of the foliation at an angle of ~30° into the rootless core of the fold packet. Figure 9(e) represents attitudes of the dominant slip foliation at sites where RSC has been measured; the greatest concentration of points is the pole to the plane oriented 058° 86°N. Based on these measurements RSC developed at a counterclockwise angle of 28° to the orientation of the dominant slip foliation.

The locations where measurements of NSC surfaces were made are shown in Fig. 7(e), and the corresponding synoptic plot of these data are shown in Fig. 9(b). NSC is preferentially developed in micaceous metasedimentary

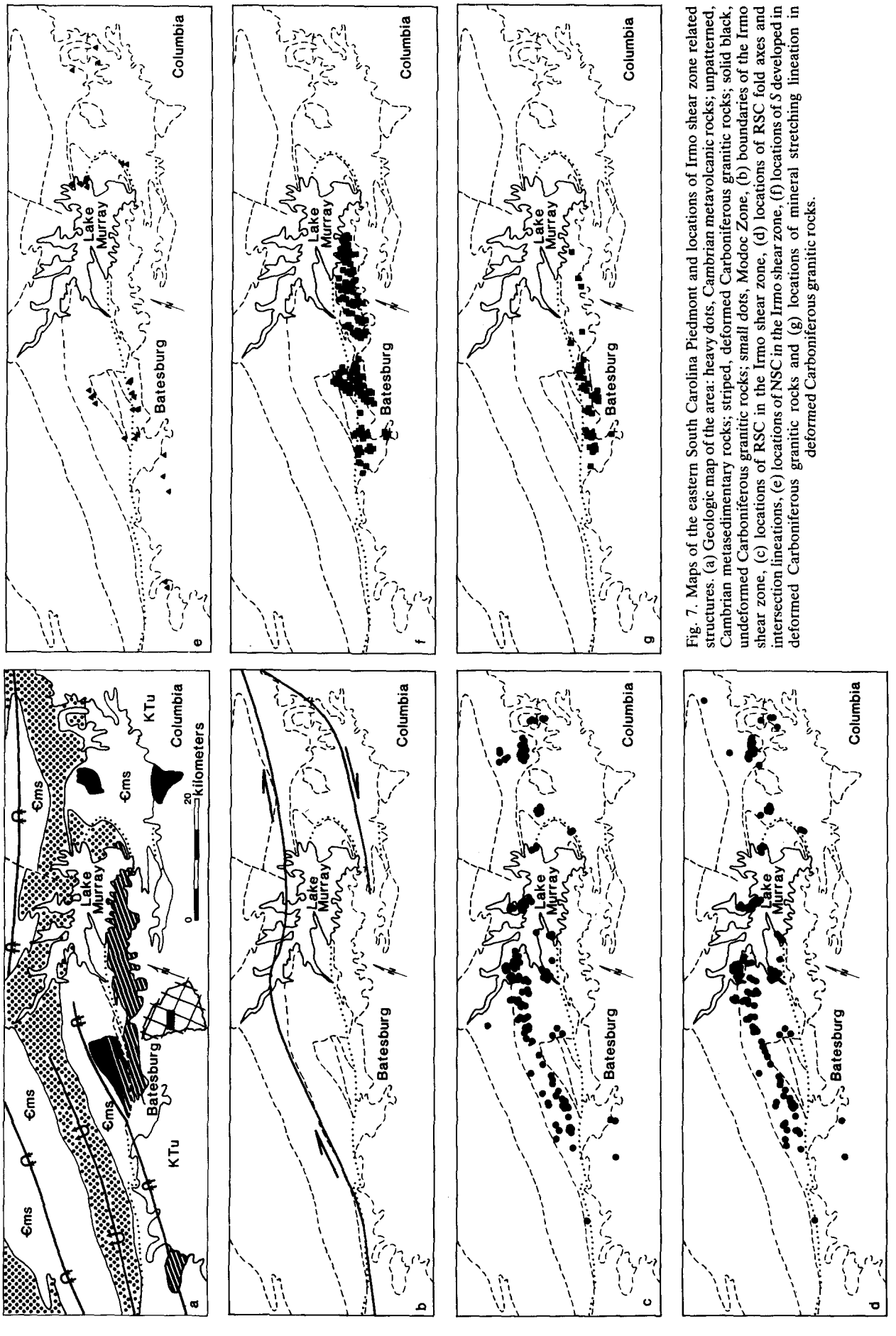

Fig. 7. Maps of the eastern South Carolina Piedmont and locations of Irmo shear zone related structures. (a) Geologic map of the area: heavy dots, Cambrian metavolcanic rocks; unpatterned, Cambrian metasedimentary rocks; striped, deformed Carboniferous granitic rocks; solid black, undeformed Carboniferous granitic rocks; small dots, Modoc Zone, (b) boundaries of the Irmo shear zone, (c) locations of RSC in the Irmo shear zone, (d) locations of RSC fold axes and intersection lineations, (e) locations of NSC in the Irmo shear zone, (f) locations of S developed in deformed Carboniferous granitic rocks and (g) locations of mineral stretching lineation in deformed Carboniferous granitic rocks.

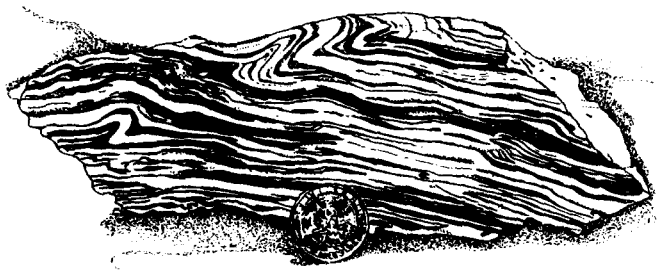

Fig. 8. Dextral-verging, rootless, intrafolial fold of RSC in flaser-bedded sandstone. Note the small flexures in the lower left and upper right. The detachment initiates in a pelitic seam and dies in the core of the fold.

rocks and in deformed Carboniferous granitic rocks. During development of the Irmo shear zone, a strong foliation (S) and lineation formed in some previously undeformed Carboniferous granitic rocks (Fig. 7f); the average orientation of this foliation is 069° 78°N (Fig. 9g). This foliation is defined by the alignment of feldspar augen and rotated and recrystallized biotite grains. NSC structures deform this foliation locally. The average orientation of the dominant slip foliation, at sites where NSC was measured, is 055° 76°N (Fig. 9f). Based on these data, NSC develops at a clockwise angle of ~35° to the dominant slip foliation. The dextral shear sense of NSC surfaces and their steeply dipping attitude indicate development in a steeply dipping dextral shear zone undergoing approximately horizontal displacement. Elongation lineations developed in the Carboniferous orthogneisses are oriented 069° 14° (Figs. 9c and 7g) suggesting a subhorizontal transport direction. These data are consistent with the other field observations indicating development in a steeply dipping, NE-trending, dextral shear zone.

While the angular and spatial relationships between RSC, NSC and folia along which slip is inferred are consistent, there is only a small variation in the average strike of dominant slip folia for NSC and RSC, ~5°. Also, RSC and NSC are sometimes observed occurring together with no apparent overprinting relationships. There are several possible explanations for such a small angle between the dominant slip foliation for RSC and NSC. (1) In general, resolved shear stresses prohibit slip on folia on all but a few planes that are subparallel to the shear zone movement direction. (2) The Irmo shear zone progressively reoriented folia, and conditions for slip on folia changed continuously during the zone's history of movement. (3) Field evidence suggests that many shear zone structures developed in zones of high strain, and strain within the shear zone is highly inhomogenous. Locally, boundary conditions and orientations of high strain zones within the Irmo shear zone are variable, and lack of continuous exposures has hindered finer resolution of this effect. (4) It is possible that RSC and NSC do not necessarily form in the same area as the folia whose slip they compensate. RSC and NSC might only indicate slip, and not that slip has occurred locally. These possible explanations are not mutually exclusive.

DISCUSSION AND CONCLUSIONS

Normal slip crenulations (NSC) and reverse slip crenulations (RSC) are here shown to be reliable and

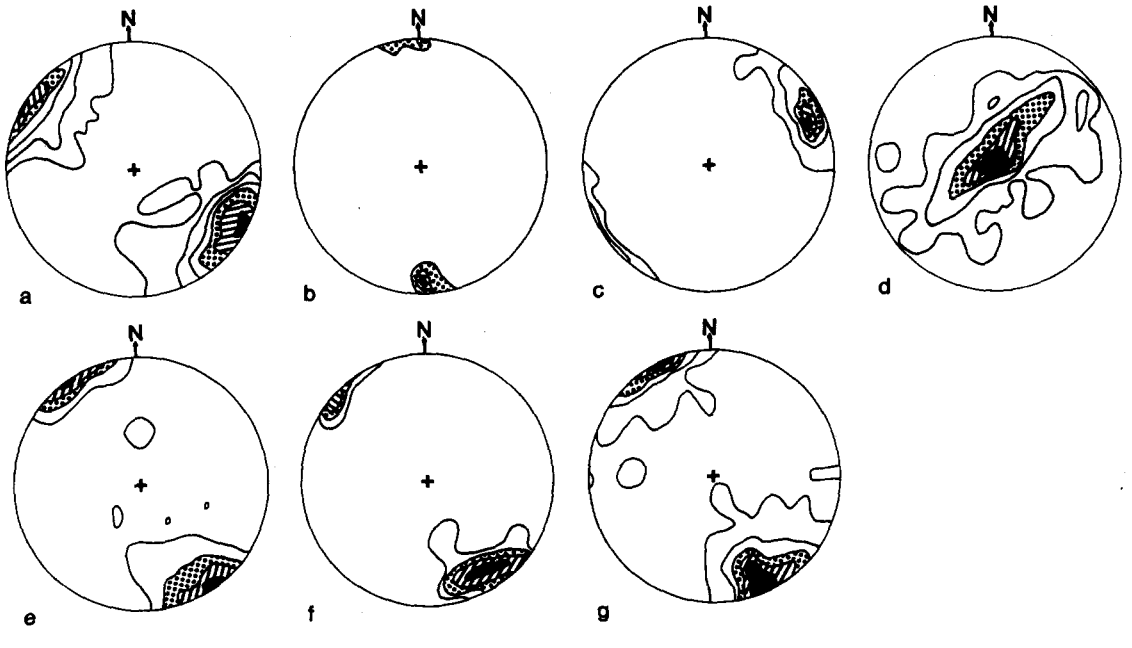

Fig. 9. Stereo-net plots of some fabric elements in the Irmo shear zone (lower hemisphere, equal-area projections): (a) 207 poles to RSC planes, contours 11, 8, 6, 4, 2%; (b) 28 poles to NSC planes, contours 30, 20, 10%; (c) 45 elongation lineations in deformed Carboniferous granitic rocks, contours 12, 9, 6, 3, 0%; (d) 218 RSC fold axes and intersection lineations, contours 10, 8, 6, 4, 2%; (e) 169 poles to dominant slip foliation at sites where RSC has been measured, contours 22, 16, 10, 4%; (f) 28 poles to dominant slip foliation at sites where NSC has been measured, contours 20, 15, 10, 5%; and (g) 262 poles to S in deformed Carboniferous granitic rocks, contours 12, 9, 6, 3, 0%.

complementary sense of shear indicators. Because their development involves slip on foliation, they indicate only the sense of shear of the slip, which may or may not relate to the deformation responsible for forming the foliation in the first place. Our data indicate that both RSC and NSC are inclined to the shear zone wall. In addition, in the Irmo shear zone there is an empirical relationship between orientations of crenulations and foliations: crenulations develop at ~30° angle to the dominant slip foliation. In our opinion, normal slip crenulations are the same or analogous to *S–C* structures (Berthé *et al.* 1979, Simpson & Schmid 1983, Lister & Snoke 1984), shear bands (White *et al.* 1980), extensional crenulation cleavage (Platt & Vissers 1980) already in the literature. We avoid using these terms in order to avoid prejudices associated with the orientation of each with respect to the shear plane and the inferred kinematic development of each, and in order to present NSC and RSC as complementary parts of an integrated system. There are several ways to generate folds in shear zones: passive amplification of perturbations (Cobbold & Quinquis 1980), compression during progressive simple shear and as a consequence of slip along foliation. Distinguishing mechanisms of shear zone-related folds in the field is difficult, and all three mechanisms may be complementary. *P*-shears (Tchalenko 1970) are possibly analogous to reverse slip crenulations. We have demonstrated relationships between pre-existing foliation and two sets of crenulations formed in the Irmo shear zone of the eastern South Carolina Piedmont. The observed angular and spatial relationships are consistent with strain compatibility. We offer RSC and NSC as geometrically defined terms for crenulations formed in shear zones. The use of these terms should not necessarily imply agreement with our inference that they form at an angle to the shear zone wall or that they form in order to compensate for components of foliation slip normal to the overall displacement direction in the shear zone.

Acknowledgements—This work was funded by NSF grant EAR82-17743. Constructive criticism by Terry Engelder, Lucian Platt, Dave Sanderson and an anonymous referee greatly improved the manuscript. The authors thank Rick Williams for helpful discussions of some matrix operations. They also thank Lori Clark and Joyce Goodwin for help in preparing the manuscript, and Rob Dennis and Terry Dennis for their help and encouragement in the field and at home.

REFERENCES

Berthé, D., Choukroune, P. & Jegouzo, P. 1979. Orthogneiss, mylonite and non-coaxial deformation of granites: the example of the South Armorican shear zone. *J. Struct. Geol.* **1**, 31–42.

Cobbold, P. R. & Quinquis, H. 1980. Development of sheath folds in shear regimes. *J. Struct. Geol.* **2**, 119–126.

Dallmeyer, R. D., Wright, J. E., Secor, D. T. Jr. & Snoke, A. W. 1986. Character of the Alleghanian orogeny in the southern Appalachians. Part II. Geochronological constraints on the tectonothermal evolution of the eastern Piedmont in South Carolina. *Bull. Geol. Soc. Am.* **97**, 1329–1344.

Lister, G. S. & Snoke, A. W. 1984. *S–C* mylonites. *J. Struct. Geol.* **6**, 617–638.

Lister, G. S. & Williams, P. F. 1979. Fabric development in shear zones: theoretical controls and observed phenomena. *J. Struct. Geol.* **1**, 283–298.

Lister, G. S. & Williams, P. F. 1983. The partitioning of deformation in flowing rock masses. *Tectonophysics* **92**, 1–34.

Passchier, C. W. 1984. The generation of ductile and brittle shear bands in a low angle mylonite zone. *J. Struct. Geol.* **6**, 273–281.

Platt, J. P. & Vissers, R. L. M. 1980. Extensional structures in anisotropic rocks. *J. Struct. Geol.* **2**, 397–410.

Secor, D. T. Jr. & Snoke, A. W. 1978. Stratigraphy, structure and plutonism in the central South Carolina Piedmont. In: *Geological Investigations in the Eastern Piedmont, Southern Appalachians* (edited by Snoke, A. W.). Columbia, South Carolina Geological Survey, Carolina Geological Society Guidebook for 1978, 65–123.

Secor, D. T. Jr., Snoke, A. W., Bramlett, K. W., Costello, O. P. & Kimbrell, O. P. 1986. Character of the Alleghanian orogeny in the southern Appalachians. Part I. Alleghanian deformation in the eastern Piedmont of South Carolina. *Bull. Geol. Soc. Am.* **97**, 1319–1328.

Simpson, C. & Schmid, S. M. 1983. An evaluation of criteria to deduce the sense of movement in sheared rocks. *Bull. Geol. Soc. Am.* **94**, 1281–1288.

Snoke, A. W., Secor, D. T., Jr., Bramlett, K. W. & Prowell, D. C. 1980. Geology of the eastern Piedmont fault system in South Carolina and eastern Georgia. In: *Excursions in Southeastern Geology* (edited by Frey, R. W.). *Falls Church, Virginia, American Geological Institute* **1**, 59–100.

Snoke, A. W. & Secor, D. T. Jr. 1983. Sense of shear on the Modoc zone, South Carolina Piedmont—Implications for late Paleozoic geodynamic scenario. *Geol. Soc. Am. Abstracts with Programs* **15**, 110.

Tchalenko, J. S. 1970. Similarities between shear zones of different magnitudes. *Bull. Geol. Soc. Am.* **81**, 1625–1640.

White, S. H., Burrows, S. E., Carreras, J., Shaw, N. D. & Humphreys, F. J. 1980. On mylonites in ductile shear zones. *J. Struct. Geol.* **2**, 175–187.